JOURNAL OF ENERGY, MATERIALS, AND INSTRUMENTATION TECHNOLOGY

Journal Webpage https://jemit.fmipa.unila.ac.id/

# Extraction of Nanocellulose from Bagasse Using Acid Hydrolysis Method

Rethanita Zaharani*, Posman Manurung, Iqbal Firdaus, Dwi Asmi and Ahmad Faruq Abdurrahman

Department of Physics, Faculty of Mathematics and Natural Sciences, University of Lampung, Bandar Lampung, Indonesia, 35141

**Article Information**

*Article history:*
*Received November 3, 2022*
*Received in revised form February 7, 2023*
*Accepted February 8, 2023*

***Keywords:*** *Nanocellulose, bagasse, acid hydrolysis, $H_2SO_4$*

**Abstract**

*The acid hydrolysis method was used to extract nanocellulose from bagasse. This study aims to prepare nanocellulose from sugarcane bagasse by acid hydrolysis method and to know the results of characterization with X-ray diffraction (XRD), Scanning Electron Microscopy (SEM), and Fourier Transform Infrared (FTIR). In this study, 4 samples were made with variations of H2SO4 of 19, 29, 39 and 45%. XRD analysis shows that with the increase of sulfuric acid, the percentage of each sample increases, but in the 39% sample, there is a decrease in purity because there are still areas of cellulose that have yet to disappear. The phase identification results show that in the sample with 19, 29, and 39% addition, $H_2SO_4$ Ia, Iß, and thenardite phases were formed. In the sample, 45% only form Ia and Iß phases with a resulting particle size of 2.83 nm and a degree of crystallinity of 55.52%. The results of the SEM test analysis show that the image pattern has stone structures that overlap each other. The results of FTIR analysis show that the functional groups detected are O – H, C – H, C ≡ C, C = C, H – C – H, C – O, and C – O – C, which indicates the presence of nanocellulose.*

**Informasi Artikel**

*Proses artikel:*
*Diterima 3 November 2022*
*Diterima dan direvisi dari 7 Februari 2023*
*Accepted 8 Februari 2023*

***Kata kunci:*** *Nanoselulosa, ampas tebu, hidrolisis asam, H2SO4*

**Abstrak**

*Telah dilakukan pembuatan nanoselulosa dari ampas tebu dengan metode hidrolisis asam. Penelitian ini bertujuan untuk mengetahui pembuatan nanoselulosa dari ampas tebu dengan metode hidrolisis asam dan mengetahui hasil dari karakterisasi dengn X- Ray Diffraction (XRD), Scanning Electron Microscopy (SEM) and Fourier Transform Infrared (FTIR). Pada penelitian ini dibuat 4 sampel dengan variasi H2SO4 yang digunakan adalah 19, 29, 39 dan 45%. Analisis XRD menunjukkan bahwa semakin besar konsentrasi H2SO4 yang digunakan maka persentase dari setiap sampel semakin meningkat tetapi pada sampel 39% terjadi penuruan kemurnian yang disebabkan masih terdapat daerah selulosa yang belum hilang. Hasil indentifikasi fasa diperoleh bahwa pada sampel dengan penambahan $H_2SO_4$ 19, 29, 39% terbentuk fasa Ia, Iß dan thenardit. Sementara, pada sampel 45% hanya terbentuk fasa Ia dan Iß dengan ukuran partikel yang dihasilakan sebesar 2,83 nm dan derajat kristalinitas sebesar 55,52%. Hasil analisis uji SEM diperoleh bahwa pola gambar memiliki struktur susunan batu yang saling beryumpang tindih. Hasil analisis FTIR menujukkan gugus fungsi yang terdeteksi yaitu O – H, C – H, C ≡ C, C = C, H – C – H, C – O, dan C – O – C yang menujukkan kehadiran nanoselulosa*

## 1. Introduction

Cellulose is the main component of the cell wall of plants and organisms (Fengel & Wegener, 1983). Cellulose is known for its insolubility in water and its resistance to various chemical treatments, with the exception of strong acids (Karlsson, 2006). Through chemical hydrolysis methods, cellulose can be transformed into nanomaterials, resulting in the production of nanocellulose.

Nanocellulose is cellulose particles with a size of less than 100 nm (Ioelovich, 2012). This is evident from the enhanced dispersion and biodegradation capabilities, along with improvements in crystallinity, aspect ratio, and

* Corresponding author.
E-mail addres: rethanitaz@gmail.com

surface area. Nanocellulose is also utilized as an additive in biodegradable products, a reinforcement material for membranes, a medium for drug delivery, and implants, as well as a thickening agent for dispersions.

Hydrolysis is a reaction between a reactant and water that results in the decomposition of a compound. Acids commonly used in hydrolysis are acetic acid, phosphoric acid, hydrochloric acid, and sulfuric acid. Hydrolysis using sulfuric acid can produce higher crystals because this acid has more hydronium ions (Martın et al., 2002). Hydrolysis using sulfuric acid showed that nanocellulose can easily disperse by water (Liu et al., 2016) and its widely regarded as one of the most efficient methods for obtaining pure cellulose materials (Thomas et al., 2022). The acid hydrolysis process occurs, and cellulose consists of amorphous and crystalline regions. The amorphous region has a lower density than the crystalline region, so when cellulose is treated with strong acid, part of the amorphous region will degrade and release the crystalline region (Mandal and Chakrabarty, 2011).

Bagasse, often referred to as sugarcane bagasse, is a by-product of sugarcane extraction. Based on data from the Indonesian Sugarcane Statistics Bureau, bagasse accounts for 32% of the total weight of sugarcane processed. (Habibullah, 2019). Bagasse fiber is insoluble in water and consists of cellulose, pentoses, and lignin. The cellulose in bagasse is coated with lignin, which makes the cellulose structure strong. Then, the bagasse needs to be dignified to remove the lignin content (Howard et al., 2003).

This study focused on extracting nanocellulose from bagasse sourced in Central Lampung Regency. The objective was to achieve the highest sample purity from locally available bagasse. The extraction process involved bleaching with NaClO, delignification, and hydrolysis. This chemical process produces Cellulose Nano Crystals (CNC) containing negatively charged sulfate groups, enhancing their dispersion in aqueous solvents (Liu et al., 2014). The resulting CNC powder was analyzed using X-Ray Diffraction (XRD) and Scanning Electron Microscopy (SEM) to evaluate its crystallinity index, crystal size, cell parameters, and morphological structure.

## 2. Research Methods

The materials used include bagasse pulp, *baicalin* textile bleach (5.25% NaClO), *Merck* 98% NaOH, *Merck* 98% $H_2SO_4$, equates, and aquabidest. First, bagasse was bleached using 5.25% NaClO and then dried in the sun. Then, 10 g of dry pulp was mixed with 100 ml of 3% NaOH and stirred at 50°C for 2 h. This stage is called delignification, which is the removal of lignin. After this stage is completed, the precipitate contained is taken and mixed with 100 ml of $H_2SO_4$ with various concentrations (19, 29, 39, and 45%) and then stirred while heating at 45°C in the open state for an hour. This acid hydrolysis step aims to remove the remaining hemicellulose and lignin with pre-cellulose Nano Crystal (p-CNC) products.

Next, p-CNC was washed using 300 ml aquabidest and neutralized with 10% NaOH until it reached pH 7. Then, the sample was dialyzed by centrifugation for 10 min until three times. The p-CNC precipitate was filtered using filter paper and dried in an oven at 100°C for 30 min at regular intervals. The final product in the form of CNC was ground using an agate mortar. The resulting CNC powder was then characterized using XRD and SEM. XRD analysis, conducted at Glabs Indonesia Utama Bandung with a Rigaku Miniflex, provided data on the crystallinity index, crystal size, and cell parameters. Meanwhile, SEM analysis was performed at FMIPA ITB with a Hitachi SU3500 instrument to examine the morphological structure of the samples.

## 3. Results and Discussions

**Figure 1** shows the results of the synthesis of bagasse through an acid hydrolysis process into CNC powder.


(a) (b) (c) (d)

**Figure 1.** CNC resulting from the hydrolysis of $H_2SO_4$ (a) 19%, (b) 29%, (c) 39%, and (d) 45%

Based on **Figure 1**, the increase of $H_2SO_4$ caused the color of the sample to darken. This is due to the presence of $H_2SO_4$plus water, which produced heat. It is well known that acid solutions have strong oxidizing properties. As a result, cellulose hydrolysis causes degradation, dehydration, and carbonization, which is the burning of cellulose carbon. This carbonation causes the color of the sample to darken (Ioelovich, 2012).

### 3.1 XRD Analysis

*1. Qualitative Analysis*

**Figure 2** shows the XRD results of the four samples. Qualitative analysis was done by matching methods between the database and XRD data. The databases used are the Crystallography Open Database (COD) of 00-411-4994 and 00-411-4382 for $I_\alpha$ and $I_\beta$, respectively (Nishiyama et al., 2002; 2003). The presence of crystalline phases of $I_\alpha$ is in the range of 15-16° and $I_\beta$ in the range of 22-23° (Mandal & Chakrabarty, 2011).

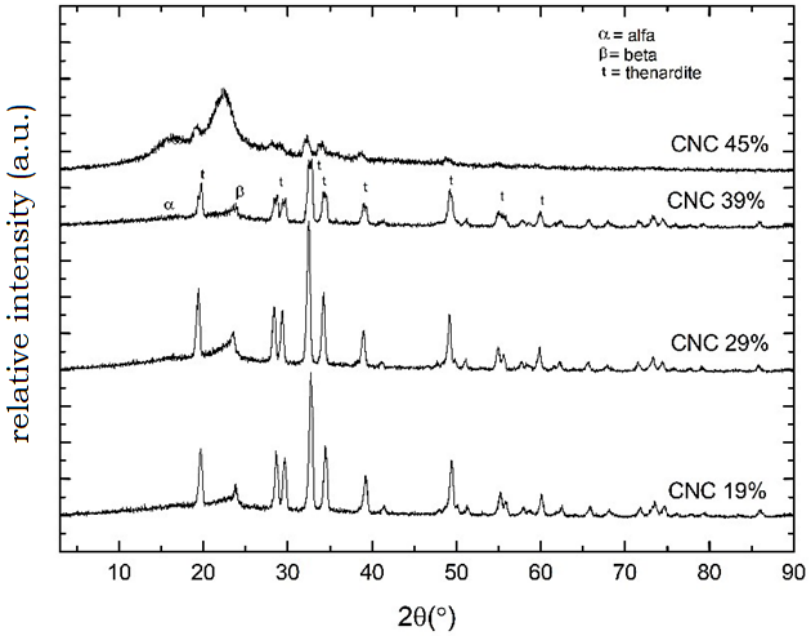


**Figure 2.** Diffractogram of nanocellulose in different sulfuric acid

Based on **Figure 2**, the purest nanocellulose diffractogram was obtained for the CNC-45% sample, which displayed only two diffraction peaks, with the maximum peak that occurs at 2θ being 22.5°. It is consistent with the results of previous studies, which found a maximum peak of 22.5° (Mandal & Chakrabarty, 2011). The level of CNC crystallinity was determined using calculations based on Equation 1.

$$I_C = \frac{I_{max} - I_{am}}{I_{max}} \times 100\% \quad (1)$$

Where $I_C$ is a crystallinity index, $I_{max}$ is the intensity of the maximum diffraction peak, and $I_{am}$ is the intensity of the amorphous baseline. The crystallinity results after using equation (1) are shown in **Table 1**.

**Table 1.** CNC crystallinity index calculation results

| Sample | $2\theta_{max}$ (°) | $I_{max}$ (cps) | $2\theta_{am}$ (°) | $I_{am}$ (cps) | $I_C$ (%) |
|---|---|---|---|---|---|
| CNC-19% | 23.81 | 170.95 | 18.54 | 100.08 | 42.45 |
| CNC-29% | 23.59 | 227.01 | 18.04 | 114.09 | 47.74 |
| CNC-39% | 23.81 | 295.87 | 18.04 | 187.74 | 36.54 |
| CNC-45% | 22.5 | 911.89 | 18.13 | 405.57 | 55.52 |

Based on **Table 1**, the highest crystallinity index is obtained in the sample CNC-45% of 55.52%. This purity percentage is below the study's results (Mandal & Chakrabarty, 2011), which showed bagasse with a CNC purity of 76%. However, the 39% CNC sample experienced a decrease in purity because there were still areas of cellulose that had not been degraded, resulting in a purity of 36.54%. A low percentage of CNC purity results in the presence of impurity phases.

Meanwhile, to calculate the size of nanocellulose crystals, Scherrer's formula is used, which is written as (Cullity, 1978):

$$L = \frac{K\lambda}{B\cos\theta} \quad (2)$$

Where $L$ is the diameter of crystal size in the nanoscale (nm), $K$ is a Scherrer's constant of 0.9, and $\lambda$ is the wavelength of the X-ray. $B$ is determined as the full width at half maximum (FWHM), and $\theta$ is the angle of the diffraction peak. The calculation result of crystal size based on XRD data can be seen in **Table 2**.

**Table 2.** CNC diameter of crystal size

| Sample | $K$ | $2\theta$ (°) | $\theta$ (°) | FWHM (rad) | $\lambda$ (nm) | $L$ (nm) |
|---|---|---|---|---|---|---|
| CNC-19% | 0.9 | 23.81 | 11.90 | 0.01 | 0.15405 | 10.82 |
| CNC-29% | 0.9 | 23.59 | 11.79 | 0.02 | 0,15405 | 6.70 |
| CNC-39% | 0.9 | 23.82 | 11.91 | 0.01 | 0.15405 | 8.92 |
| CNC-45% | 0.9 | 22.5 | 11.35 | 0.04 | 0.15405 | 2.83 |

**Table 2** displays the size of CNC particles extracted from bagasse. The 45% sample obtained the smallest size, 2.83 nm, and the largest, 10.82 nm, in the 19% sample. However, the 39% sample experienced an increase in particle

size, which was affected by the presence of impurities. This is consistent with the results of a study conducted by Ghazya et al. (2016), which produced a particle size of 2-30 nm.

*2. Quantitative Analysis*

Quantitative analysis was performed by refining the XRD data using Rietica software. Due to the database's limitations, the calculation method used is Le Bail. In this analysis, the cell parameters used were Nishiyama et al. (2002; 2003) for nanocellulose $I_\alpha$ and $I_\beta$. Meanwhile, Hawthorne used samples containing additive impurities for thenardite (COD: 00-900-4092) (Hawthorne & Ferguson, 1975). The results of data refinement are shown in **Figure 3**.

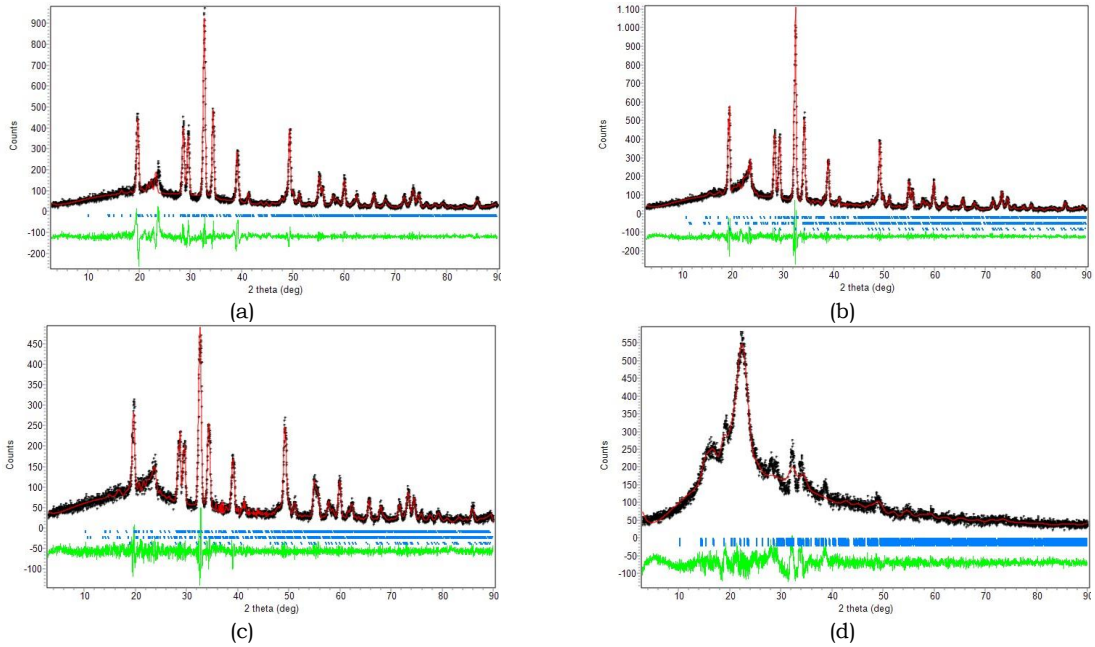


**Figure 3.** XRD data refinement results (a) CNC-19%, (b) CNC-29%, (c) CNC-39%, and (d) CNC-45%

Based on **Figure 3**, only the sample of CNC-45% contains two phases of $I_\alpha$ and $I_\beta$. Sample of CNC-19% and CNC-29% contain an additional phase of thenardite (Hawthorne & Ferguson, 1975). These can be explained through the data in **Table 3**.

**Table 3.** CNC phase parameters in molar percent (%M)

| Sample | $I_\alpha$ (%M) | $I_\beta$ (%M) | Thenardite (%M) |
|---|---|---|---|
| CNC-19% | 4.58 ± 0.00 | 17.97 ± 0.00 | 77.46 ± 0.00 |
| CNC-29% | 4.753 ± 0.00 | 17.92 ± 0.01 | 77.43 ± 0.02 |
| CNC-39% | 4.65 ± 0.00 | 17.97 ± 0.01 | 77.37 ± 0.03 |
| CNC-45% | 19.59 ± 0.27 | 80.41 ± 0.21 | - |

**Table 3** The CNC-39% sample contains only two phases of crystalline cellulose in form $I_\alpha$ and $I_\beta$, which shows the diffractogram's accuracy in **Figure 2**. Meanwhile, CNC samples 19, 29, and 39% show the presence of an additional new crystalline phase of thenardite ($Na_2SO_4$). Thenardite is a crystalline phase obtained from sodium sulfate salt-free water molecules by mixing the removed NaOH solution with the hydrolysis of $H_2SO_4$ (Thenard, 1825). The molar percentage of $I_\beta$ is approximately four times that of $I_\alpha$, which proves the degradation of $I_\alpha$ to $I_\beta$ through the hydrolysis process (Wada & Okano, 2001).

To verify that the diffractogram refinement of the CNC-45% sample yields cell parameters consistent with the Nishiyama models, the calculation of value shifts or relative errors is presented in **Table 3-4**.

**Table 4.** $I_\alpha$ phase cell parameters

| Sample | a (Å) | b (Å) | c (Å) | α (°) | β (°) | γ (°) |
|---|---|---|---|---|---|---|
| Model | 6.717 | 5.962 | 10.400 | 118.08 | 114.80 | 80.37 |
| CNC-39% | 6.648 | 5.810 | 10.187 | 117.21 | 113.80 | 81.06 |
| RE (%) | 1.678 | 1.289 | 1.034 | 0.368 | 0.436 | 0.04 |

**Table 5.** $I_\beta$ phase cell parameters

| Sample | a (Å) | b (Å) | c (Å) | α = β (°) | γ (°) |
|---|---|---|---|---|---|
| Model | 7.784 | 8.201 | 10.380 | 90.00 | 96.50 |
| CNC-39% | 7.784 | 8.201 | 10.379 | 90.00 | 96.50 |
| RE (%) | 0.00 | 0.00 | 0.570 | 0.00 | 0.00 |

**Table 4-5** shows the results of calculating the relative error (RE) between the cell parameters of the $I\alpha$ and $I\beta$ phase model with a sample CNC of 45%. All RE values are below 2%, indicating that CNC -45% cell parameter values follow Nishiyama et al.'s model (2002; 2003).

### 3.2 SEM Analysis

SEM characterization was carried out to determine the appearance of the nanostructure morphology of the CNC-45% sample, as shown in **Figure 4**.

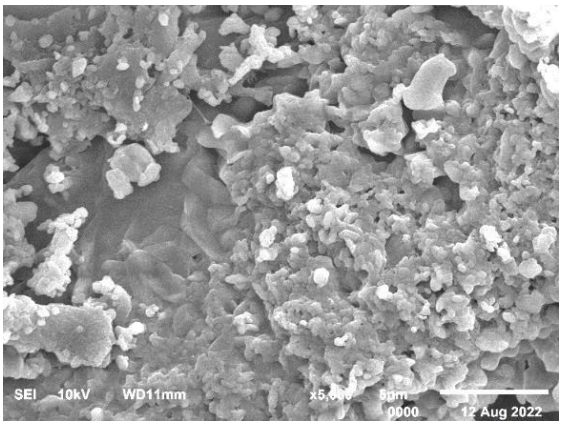


**Figure 4.** SEM observation of sample CNC-45%

Based on **Figure 4**, the morphology of CNC-45% has an overlapping structure resembling a stone arrangement. Agglomeration occurs, which prevents the measurement of the distribution of nanocellulose particles from being carried out. This overlapping structure also causes $I_\alpha$ and $I_\beta$ phase particles indistinguishable from each other (Rosanti, 2020).

### 3.3 FTIR Analysis

In order to determine the functional groups of the samples, FTIR characterization was carried out with the results shown in **Figure 5**.

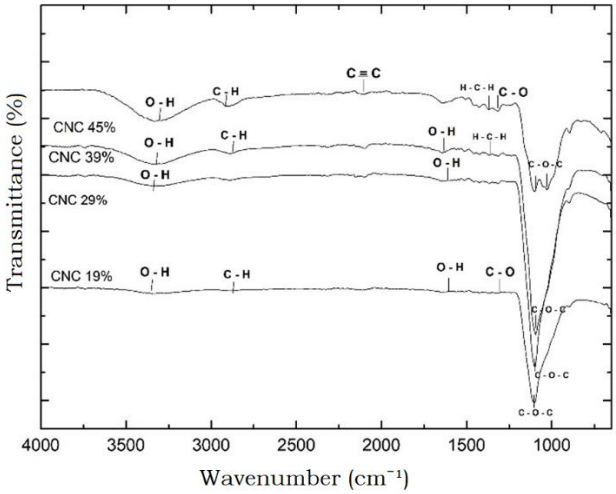


**Figure 5.** FTIR spectra of CNC samples

**Figure 5** shows that the spectra of the CNC-39% sample have the sharpest absorption regions, which are determined by the low transmittance value. Because the transmittance value is the opposite of the absorption value, it indicates that many functional groups are detected in a certain wave number. The names of the functional groups detected are shown in **Table 6** (Libretexts, 2022).

**Table 6.** $I_\beta$ phase cell parameters

| Wave number ($cm^{-1}$) | | | | Functional groups | | References |
|---|---|---|---|---|---|---|
| **CNC-19%** | **CNC-29%** | **CNC-39%** | **CNC-45%** | | | |
| 3347.1 | 3332.2 | 3332.2 | 3339.7 | O−H | Hydroxyl | (Pan et al., 2013) |
| 2892.4 | - | 2892.4 | 2914.8 | C−H | Aliphatic | (Gond et al., 2016) |
| - | - | - | 2102.2 | C≡C | Alkyne | (Coates, 2000) |
| 1647.5 | 1640 | 1640 | 1640 | O−H | Hydroxyl | (Pan et al., 2013) |
| - | - | 1423.8 | 1423.8 | H−C−H | Methylene | (Ghazya et al., 2016) |
| - | 1312 | - | 1319.5 | C−O | Aryl carbonyl Lignin | (Mandal and Chakraberty, 2011) |
| 1103.3 | 1103.3 | - | 1103.3 | C−O−C | Pyranose | (Garside and Wyeth, 2003) |
| - | - | 10.95 | 1028.7 | C−O−C | Pyranose | (Garside and Wyeth, 2003) |

Based on **Table 6**, five functional groups always be in the sample. The hydroxyl group indicates the strong interaction between cellulose and water molecules (Pan et al., 2013), while the aliphatic is part of lignocellulose (Gond et al., 2016). The next group detected is aryl carbonyl from the lignin compound (Mandal & Chakraberty, 2011). Meanwhile, pyranose is the last detected group that indicates the increase of crystallinity of nanocellulose (Garside & Wyeth, 2003).

## 4. Conclusions

The acid hydrolysis method, using various concentrations of 19, 29, 39, and 45%, has successfully produced nanocellulose from bagasse (bagasse). The XRD analysis revealed that nanocellulose extracted from bagasse achieved a purity level of 55.52% with a particle size of 2.83 nm. SEM analysis showed that the nanocellulose particles were distributed in a structure resembling overlapping stacked stones. FTIR analysis identified the presence of functional groups, including OH, CH, C≡C, HCH, CO, and COC, in the nanocellulose.

## 5. References

Cullity, B. D. (1978). *X-Ray Elements*. Department of Metallurgical Engineering and Materials Science. Addison Wesley Publishing Company. Boston. 44-500.

Coates, J. (2000). Infrared Spectral Interpretation A Practical Approach. *Encyclopedia of Analytical Chemistry*. 814.

Fengel, D. & Wegener, G. (1983). *Chemical Ultrastructure of Wood, Reactions*. Beryl. Germany: Walter de Gruyter. 421-432.

Garside, P., & Wyeth, P. (2003). Identification of Cellulose Fibers by FTIR Spectroscopy: Analysis of yarns and single fibers by total attenuated reflectance. *Studies in Conservation*. 48(4). 269–275.

Ghazy, M. B., Esmail, F. A., El-Zawawy, W. K., Al-Maadeed, M. A., & Owda, M. E. (2016). Extraction and characterization of Nanocellulose obtained from sugarcane bagasse as agro-waste. *Journal of Advances in Chemistry, pp.* 12, 4256–4264.

Gond, R. K., Gupta, M. K., & Jawaid, M. (2021). Extraction of Nanocellulose from Bagasse and its Characterization for Potential Applications. *Journal of Polymer Composites*. 2–18.

Habibullah, M. (2019). *Indonesian Sugarcane Statistics* 2018. BPS RI. Jakarta. 24–36.

Hawthorne, F.C., & Ferguson, R.B. (1975). Anhydrous Sulfate I: Refinement of the Celestite Crystal Structure with an Appendix on Thenardite Structure. *Canadian mineralogist.* 13(2). 181-187.

Howard, R.L., Abotsi, E., Jansen van Rensburg, E.L. & Howard, S. (2003) Lignocellulose Biotechnology: Issues of Bioconversion and Enzyme Production. *African Journal of Biotechnology*, 2, 602-619. http://dx.doi.org/10.5897/AJB2003.000-1115

Karlsson, H. (2006). *Fiber Guide: Fiber Analysis and Process Applications in the Pulp and Paper Industry*. Sweden: AB lorentzen and Wettre. 100–108.

Loelovich, M. (2012). Study of the Interaction of Cellulose with Concentrated Sulfuric Acid Solutions. ISRN *Chemical Engineering*. 1–7.

Martin, C., Galbe, M., Wahlbom, C.F., Hahn-Hägerdal, B., & Jönsson, L.J. (2002). Ethanol Production from Sugarcane Bagasse Enzymatic Hydrolyzate Using Saccharomyces Cerevisiae using Recombinant Xylose. *Microbial Enzymes and Technology*. 31(3). 274–282

Liu, C., Li, B., Du, H., Lv, D., Zhang, Y., Yu, G., Mu, X., & Peng, H. (2016). Properties of Nanocellulose Isolated from Corn Cob Waste Using Sulfuric Acid, Formic Acid, Oxidative and Mechanical Methods. *Carbohydrate Polymers*. 16.1-30.

Mandal, A., & Chakrabarty, D. (2011). Isolation of Nanocellulose from Waste Sugarcane Bagasse (SCB) and its Characterization. *Carbohydrate Polymers*, 86(3). 1291–1299.

Nishiyama, Y., Sugiyama, J., Chanzi, H., & Langan, P. (2002). Crystal Structure and Hydrogen Bonding System in Cellulose Iβ from Synchrotorn X-rat and Neutron Fiber Diffraction, *America Chemical Society*. 124(31). 9076.

Nishiyama, Y., Sugiyama, J., Chanzi, H., & Langan, P. (2003). Crystal Structure and Hydrogen Bonding System in Cellulose Iα from Synchrotorn X-rat and Neutron Fiber Diffraction, *American Chemical Society*. 125(47). 14301.

Pan, M., Zhou, X., & Chen, M. (2013). Cellulose Nanowhisker Isolation and Properties from Acid Hydrolysis Combined with High Pressure Homogenization. *Bioresources*, 8(1),933–943.

Rosanti, A. D., Wardani, A. R. K., & Anggraeni, H. A. (2020). Pengaruh Suhu Kalsinasi terhadap Karakteristik dan Aktivitas Fotokatalis N/TiO2 pada Penjernihan Limbah Listrik Batik Tenun Ikat Kediri. *Cakra Kimia* 8(1) 30

Thomas, S. K., Begum, P. M. S., Dominic, C. D. M., Salim, N. V., Hameed, N., Rangappa, S. M., Siengchin, S. & Parameswaranpillai, J. (2021). Isolation and characterization of cellulose nanowhiskers from Acacia caesia plant. *Journal of Applied Polymer Science*, *138*(15), 50213.

Wulandari, W. T., Rochliadi, A., & Arcana, I. M. (2016). Nanocellulose Prepared by Acid Hydrolysis of Cellulose Isolated from Sugarcane Bagasse. *IOP Conference Series: Materials Science and Engineering*, 107(1).

Wada, M., & Okano, T. (2001). Localization of Iα and Iβ Phases in Algal Cellulose Revealed by Acid Treatment. Cellulose, 8(3), 183–188.